ELSEVIER

Journal of Power Sources 54 (1995) 46–51

JOURNAL OF POWER SOURCES

Modeling the performance of rechargeable lithium-based cells: design correlations for limiting cases

Marc Doyle, John Newman

Department of Chemical Engineering, University of California, Berkeley, CA 94720, USA
Energy and Environment Division, Lawrence Berkeley Laboratory, University of California, Berkeley, CA 94720, USA

Abstract

We use simplified models based on porous-electrode theory to describe the discharge of rechargeable lithium batteries and derive analytic expressions for the cell potential, specific energy, and average power in terms of the relevant system parameters. The resulting theoretical expressions are useful for design and optimization purposes and also can be used as a tool for the identification of system limitations from experimental data. The system treated is an ohmically-limited cell with no concentration gradients having an insertion reaction whose open-circuit potential depends linearly on state-of-charge. Although the slope of the open-circuit potential controls the reaction distribution in the porous electrode, we find that the cell potential is independent of this slope. The results are applied to a cell of the form Li|polymer|$Li_yMn_2O_4$ in order to illustrate their utility.

Keywords: Rechargeable lithium batteries

1. Introduction

Rechargeable batteries based on solid lithium and lithium-ion cells have successfully penetrated the consumer market and are under consideration for electric-vehicle applications. Mathematical modeling efforts at this stage are focused on optimization of the cell design and system parameters and the thermal control of the battery module. General models have been developed to simulate the behavior of these systems during charge, discharge, and relaxation [1–3]. However, due primarily to their generality, these models are complicated, and it is often the case that for particular systems a simplified treatment is possible that captures the essential features of the discharge behavior. In these cases, one can find analytic expressions for the energy and power densities of the system as a function of the relevant parameters that characterize the system. This can greatly simplify the design process because it may reduce the problem to a single or small number of dimensionless parameters and obviate the need for numerical simulations.

There has also been some interest in the past in obtaining capacity–rate and energy–power expressions for both primary [4] and secondary [5,6] batteries. These correlations are useful as both a design tool and a method for predictions of battery performance under different operating conditions. Usually these correlations are obtained from the analysis of experimental data, and functional fits are developed that are based on empirically defined parameters with vague theoretical meaning. The method that we pursue, on the other hand, begins with the full theoretical description of the single cell and makes simplifying assumptions to reduce the problem to limiting forms that allow correlations to be developed. In this way we can obtain expressions for the parameters that appear in the correlations in terms of fundamental physical properties and system specifications. Also, having started with the general mathematical description, we can develop criteria for deciding when these limiting cases are applicable.

We consider a limiting model that is believed to be applicable to specific systems discussed in the literature. This model is applicable to systems in the absence of concentration gradients. The salt concentration is uniform, for example, with a system having a unity transference number [7] for the lithium ion or at very short times, much less than the diffusion time. If this is the case, the governing equations are much simpler, and several possibilities exist for the examination of approximate analytic solutions [8]. When concentration gradients cannot be neglected, the situation is much more complex due to the coupled nature of the governing equations. For this reason, very few analytic solutions can be found in the literature that include concentration variations in the solution phase; this problem is generally relegated to numerical methods.

SSDI 0378-7753(94)02038-5

We consider the former case, in which the solution-phase concentration is uniform over the time of discharge of the battery. We will assume that kinetic and solid-phase diffusion limitations do not exist. In addition, we will focus on a system having a single insertion electrode. The generalization of the results to a lithium-ion cell which employs two different insertion electrodes should be straightforward. With these assumptions, the system becomes similar to an ohmically-dominated porous-electrode model [9]. The reaction moves through the electrode as a front which consumes all of the available active material at a point before moving on. This situation has been the object of previous study; our contribution here is to include the effect of an open-circuit potential that depends on the state-of-charge of the electrode, as in insertion compounds. A similar problem to the one above has been considered by Atlung et al. [10,11]. However, their treatment is different from the present model, and it will be shown that the two models may apply to different times in the discharge.

The primary goal of this work will be to obtain an expression for the specific energy of the system as a function of the average specific power (Ragone plot). From this information, one can approach practical design issues such as optimal electrode thicknesses and porosities.

2. Theoretical development

We treat one-dimensional transport through the cell sandwich shown in Fig. 1. The development is based on porous-electrode theory [12], where the electrode is treated as two superimposed continua without regard for the actual geometric detail of the pore structure. The separator consists of either an inert polymer material or a nonaqueous liquid that acts as the solvent for a lithium salt. The negative electrode is a lithium foil, and the positive electrode is a porous electrode consisting of solid insertion material particles, inert conducting filler, and the solution phase. The porous electrode is assumed to have a very large electronic

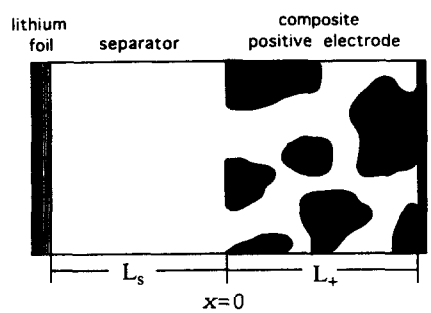

Fig. 1. Lithium/polymer cell sandwich, consisting of lithium foil negative electrode, solid polymer electrolyte, and composite positive electrode.

conductivity ($\sigma \gg \kappa$) and a large exchange current density for the insertion process. Additionally, we neglect diffusion limitations inside of the solid electrode particles; this is valid for $S_e \ll 1$, where:

$$S_e = \frac{R_s^2 I}{D_s F(1-\epsilon)c_T L_+} \tag{1}$$

These conditions have been demonstrated to hold for typical lithium insertion electrodes under a three-hour discharge [2].

The neglect of concentration gradients represents a great simplification in the theoretical treatment. This assumption will hold for any system with a unity transference number for the lithium ion; several polymer electrolytes have been developed that fulfill this condition [7]. With this assumption, as well as those given previously, the system is ohmically-dominated. The insertion reaction moves through the porous electrode like a spike, consuming all of the active material before moving on. This continues until either the cutoff potential is reached or the active material is completely consumed.

We begin by assuming that the open-circuit potential of the insertion material is a linear function of the active material utilization:

$$U = U^\theta - \frac{Q}{q} k(U^\theta - V_c) \tag{2}$$

Here we take Q to be the integral over time of the local transfer current density and q is the capacity density (C/m^3). Thus, at full discharge $Q=q$. The parameter k will vary between 0 and 1, with $k=0$ for a constant open-circuit potential and $k=1$ for a material which reaches the cutoff potential exactly at full discharge. Larger values of k are unnecessary because otherwise the maximum capacity is limited by the cutoff potential. We imagine a reaction zone of a finite thickness that moves through the porous electrode; the position of the rear edge is $x=x_r$. That is, that portion of the electrode for which $x<x_r$ has been completely consumed ($Q=q$). As we have assumed an essentially reversible insertion process, local equilibrium prevails, and:

$$U = \Phi_1 - \Phi_2 \tag{3}$$

The solid-phase potential, Φ_1, is a constant due to the large electronic conductivity.

For a quasi-steady reaction zone moving through the electrode under a galvanostatic discharge, the velocity of the zone will be I/q. We wish to find an expression for the position of this front as a function of time. The local transfer current density is related to the divergence of the current flow in the solution phase through:

$$aFj_n = \frac{\partial i_2}{\partial x} \tag{4}$$

Thus, from the definition of Q:

$$\left(\frac{\partial Q}{\partial t}\right)_x = -\left(\frac{\partial i_2}{\partial x}\right)_t \tag{5}$$

The solution-phase potential measured with a lithium reference electrode in the absence of a concentration gradient is given by Ohm's law:

$$i_2 = -\kappa \frac{\partial \Phi_2}{\partial x} \tag{6}$$

Using Eqs. (2) and (3) this becomes:

$$i_2 = -\frac{\kappa k(U^\theta - V_c)}{q} \frac{\partial Q}{\partial x} \tag{7}$$

Then, differentiating Eq. (6) with respect to either time or distance, we find that both Q and i_2 obey the same second-order partial differential equation:

$$\frac{\partial Q}{\partial t} = \frac{\kappa k(U^\theta - V_c)}{q} \frac{\partial^2 Q}{\partial x^2} \tag{8}$$

and:

$$\frac{\partial i_2}{\partial t} = \frac{\kappa k(U^\theta - V_c)}{q} \frac{\partial^2 i_2}{\partial x^2} \tag{9}$$

If the electronic conductivity were not infinite, one would need to replace κ with $\sigma\kappa/(\sigma+\kappa)$ in Eqs. (8) and (9).

We can solve Eq. (9) subject to the following boundary conditions:

$$i_2 = I \text{ for } (x < x_r) \tag{10}$$

and:

$$i_2 = 0 \text{ at } (x = \infty) \text{ and } (t = 0) \tag{11}$$

These boundary conditions result from the reaction zone assumption. If we transform Eq. (9) by defining a new coordinate that moves with the reaction zone:

$$X = x - \frac{It}{q} \tag{12}$$

then in terms of this new variable the differential equation becomes:

$$\frac{\partial i_2}{\partial t} = \frac{I}{q} \frac{\partial i_2}{\partial X} + \frac{\kappa k(U^\theta - V_c)}{q} \frac{\partial^2 i_2}{\partial X^2} \tag{13}$$

This has a solution of the form:

$$i_2 = A \exp(BX) \tag{14}$$

Substitution into Eq. 13 leads to the condition that:

$$B = 0 \text{ or } B = \frac{-I}{\kappa k(U^\theta - V_c)} \tag{15}$$

Since $i_2 = 0$ as X approaches ∞, we use the second value of B only. This boundary condition should rigorously be applied at some finite value of X, but the problem is not tractable unless one makes the assumption that $X \to \infty$, meaning that the reaction zone is thin compared with the electrode thickness. This assumption will be less valid for very thin electrodes where a larger fraction of the active material is near the electrode/current collector boundary. One can see here the difficulty of treating a system with a finite electronic conductivity; then two reaction zones would move from either boundary inward towards the center of the electrode [9].

Next, as we know that the current density is equal to the cell current at the rear of the reaction zone, we write Eq. (14) as:

$$i_2 = I \exp\left(-\frac{I(x - x_r)}{\kappa k(U^\theta - V_c)}\right) \text{ for } x > x_r \tag{16}$$

$$i_2 = I \text{ for } x < x_r \tag{17}$$

Here, we have written i_2 in terms of the still unknown value of x_r. One finds from Eq. (16) that the effect of the sloping open-circuit potential function is to spread out the reaction zone; as k approaches 0 the reaction zone becomes a delta function at $x = x_r$. With the current density known, Ohm's law can be integrated to find the distribution of the potential in the solution phase:

$$\Phi_2 = \Phi_2(\infty) + k(U^\theta - V_c) \exp\left(-\frac{I(x - x_r)}{\kappa k(U^\theta - V_c)}\right) \tag{18}$$

Hence, the utilized capacity is:

$$Q = q \exp\left(-\frac{I(x - x_r)}{\kappa k(U^\theta - V_c)}\right) \text{ for } x > x_r \tag{19}$$

$$Q = q \text{ for } x < x_r \tag{20}$$

The overall charge balance can then be used to find x_r:

$$\int_0^\infty Q \, dx = It = qx_r + \frac{q\kappa k(U^\theta - V_c)}{I} \tag{21}$$

Thus,

$$x_r = \frac{It}{q} - \frac{\kappa k(U^\theta - V_c)}{I} \tag{22}$$

At short times Eq. (22) gives an apparently negative reaction zone position. This is due to an initial transient period during which the capacity at the front of the electrode has not yet been exhausted. Our analysis does not apply during this period.

Fig. 2 shows the distribution of utilized capacity across the porous electrode using Eqs. (19) and (22), for various values of k. As k increases, the open-circuit

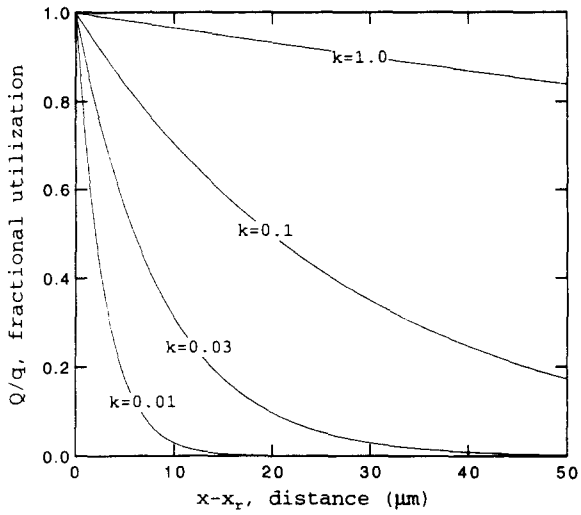

Fig. 2. The distribution of utilized capacity across the reaction zone. Various values of k, the slope of the open-circuit potential vs. state-of-charge, are used to demonstrate the effect of this parameter on the current distribution.

potential becomes more sloped, and the reaction zone becomes more diffuse. For large enough values of k, the reaction is taking place throughout the electrode; the reaction-zone assumption is then no longer valid. In order for the 'thick cell' assumption to hold, one requires that the utilized capacity drops essentially to zero before the back of the electrode is reached. This is obviously not the case for the $k=1$ or $k=0.1$ curves, but does appear to hold for the other values of k. The reaction-zone thickness is also inversely proportional to the superficial cell current density I and proportional to the conductivity κ. The values of other parameters used in this Figure are from the model Li/Mn_2O_4 system described in the Appendix.

Now we can seek an explicit expression for the cell potential, and from this, the specific energy. The distribution of potentials in the cell is:

$$\Phi_2(\text{neg}) - \Phi_2(x=0) = \frac{IL_s}{\kappa_s} \tag{23}$$

$$\Phi_2(x=0) - \Phi_2(x=x_r) = \frac{Ix_r}{\kappa} \tag{24}$$

$$\Phi_2(x=x_r) - \Phi_2(\infty) = k(U^\theta - V_c) \tag{25}$$

$$\Phi_2(\infty) - \Phi_1 = -U^\theta \tag{26}$$

We can arbitrarily take the potential at the negative electrode to be zero, $\Phi_2(\text{neg})=0$, and then the cell potential is given by summing the potentials across the cell:

$$V = U^\theta - k(U^\theta - V_c) - I\left(\frac{L_s}{\kappa_s} + \frac{x_r}{\kappa}\right) \tag{27}$$

Using the definition of x_r, this becomes:

$$V = U^\theta - \frac{IL_s}{\kappa_s} - \frac{I^2 t}{\kappa q} \tag{28}$$

Notice that the cell potential is independent of the value of k [13]. A plot of the cell potential versus time for various discharge rates is given as Fig. 3.

Setting the cell potential in Eq. (28) equal to the cutoff potential determines the time of discharge:

$$t_d = \frac{\kappa q}{I^2}\left(U^\theta - V_c - \frac{IL_s}{\kappa_s}\right) \tag{29}$$

Integration of the instantaneous power delivered over the time of discharge gives the energy:

$$E = \int_0^{t_d} IV\,dt = It_d\left(U^\theta - \frac{IL_s}{2\kappa_s} - \frac{(U^\theta - V_c)}{2}\right) \tag{30}$$

Substitution of t_d from Eq. (29) gives:

$$E = \frac{\kappa q}{2I}\left(U^\theta - V_c - \frac{IL_s}{\kappa_s}\right)\left(U^\theta + V_c - \frac{IL_s}{\kappa_s}\right) \tag{31}$$

These expressions can be used to calculate the average specific power available. The average specific power is:

$$P = E/t_d = \frac{I}{2}\left(U^\theta + V_c - \frac{IL_s}{\kappa_s}\right) \tag{32}$$

Eqs. (31) and (32) are written on a per-unit-area basis and thus should be divided by the mass per unit area of the cell:

$$M = \rho_s L_s + [\epsilon\rho_s + (1-\epsilon)\rho_+]L_+ \tag{33}$$

which as written accounts for positive electrode and separator masses only, but could also include other masses in the system.

Eqs. (31) and (32) are the basis for a Ragone plot given as Fig. 4. The system under consideration, de-

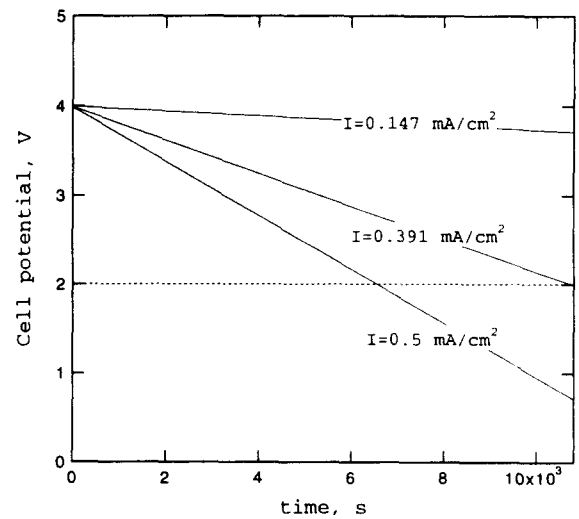

Fig. 3. Cell potential for various values of the current density during a galvanostatic discharge. The dashed line is the cutoff potential.

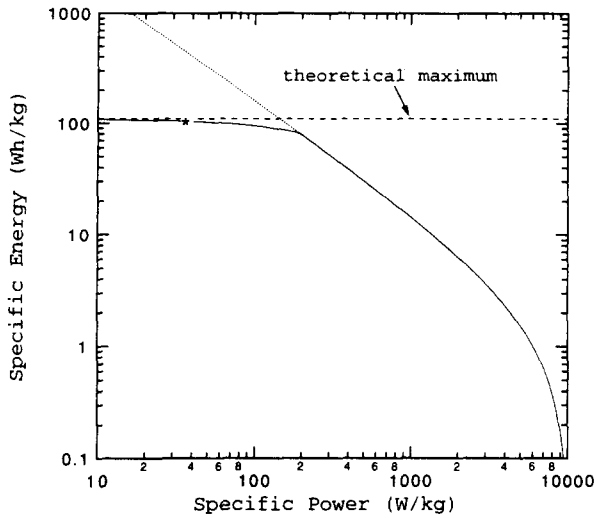

Fig. 4. Ragone plot of specific energy vs. specific power for the manganese dioxide system. The dotted line is the prediction of the reaction-zone model, and the dashed line is the maximum specific energy based on the total capacity of the cell. The solid line results from combining the reaction-zone model with a maximum capacity condition.

scribed in the Appendix, is a lithium/manganese dioxide cell with a solid polymer electrolyte. The dashed line in Fig. 4 indicates the maximum specific energy (112 Wh/kg) that the system can provide, calculated from the initial capacity. The relatively low maximum specific energy found for this system (compared with the theoretical maximum of approximately 478 Wh/kg) is due to the small range of capacity over which the manganese dioxide electrode is imagined to be used ($0.6 \leqslant y \leqslant 0.8$ in $Li_yMn_2O_4$) in this model. Notice that a substantial portion of the Ragone plot is predicted to have a slope of -1. At very high values of the specific power, the maximum power is approached, and the curve bends over and becomes vertical.

The reaction-zone model predicts that the specific energy attainable continues to increase at lower values of the specific power because of the thick-cell assumption which inherently neglects the finite amount of active material in the cell. This result is illustrated by the dotted line in Fig. 4. However, the specific energy should bend over at lower rates and approach the maximum specific energy indicated in the Figure. Thus, the solid curve in Fig. 4 uses Eq. (30) to calculate the specific energy with the modification that the discharge time is not allowed to exceed the total capacity of the electrode at the given rate. The discharge time is chosen to be the lower of Eq. (29) and:

$$t_d = \frac{qL_+}{I} \tag{34}$$

This is the expected behavior of the Ragone plot.

The equations given above could be used as tools for the optimization of adjustable system parameters, primarily component thicknesses and volume fractions. A procedure for this is given in the literature [13]. By maximizing the specific energy with respect to the discharge rate, with the discharge time fixed (e.g., 3 h), one finds that the optimum values are $\epsilon = 0.14$ and $L_+/L_s = 4$, for this example. Thicker and less porous electrodes are typical for a system optimized for a long discharge time. These values were used to produce Figs. 2 to 4, and the value of the specific energy for the three-hour discharge rate is indicated with a marker in Fig. 4. The optimum operating point is near to, but not quite at, the break in the Ragone plot, which is the usually expected result. The optimization procedure is more complicated if additional battery masses are included in Eq. (33).

In the work of Atlung and co-workers [10,11] an equation analogous to our Eq. (8) is solved using the boundary conditions:

$$\frac{\partial Q}{\partial x}(t, x=0) = -\frac{Iq}{\kappa k(U^\theta - V_c)} \text{ and}$$

$$\frac{\partial Q}{\partial x}(t, x=L_+) = \frac{Iq}{\sigma k(U^\theta - V_c)} \tag{35}$$

However, as the authors point out, these boundary conditions are not truly valid and instead a moving-zone boundary condition should apply as was used in this work. These boundary conditions on Q apply up until such time that the capacity at the front of the electrode is exhausted, suggesting that this approach may be valid during the initial transient period not covered above (see Eq. 22). Indeed, Atlung and co-workers [10,11] find good agreement between experimental data and theoretical predictions at short times into the discharge where a $t^{1/2}$ dependence of cell potential on time is expected rather than the t dependence found above.

3. Conclusions

A simplified model of an ohmically-dominated porous electrode with no diffusion or kinetic limitations is developed. The open-circuit potential of the electrode reaction depends linearly on the state-of-charge of the electrode, as in several commonly used insertion materials. The model is used to derive analytic expressions for the specific energy and average specific power that are attainable. The sloping open-circuit potential brings about a more uniform reaction distribution in the porous electrode but does not enter into the cell potential. These equations are useful in optimization procedures and can be used as a guide for the correlation of experimental data. The formulas have been applied to a lithium/manganese dioxide system to illustrate their consequences.

4. List of symbols

a specific interfacial area (m^2/m^3)
c_T maximum concentration in solid (mol/m^3)
D_s diffusion coefficient of lithium in the solid electrode particles (m^2/s)
F Faraday's constant (96 487 C/eq)
i_1 electronic current density in the solid phase (A/m^2)
i_2 ionic current density in the solution phase (A/m^2)
I superficial current density (A/m^2)
j_n pore wall flux of lithium ions ($mol/(m^2\ s)$)
k slope of open-circuit potential
L cell thickness (m)
q charge density of composite positive electrode (C/m^3)
Q integral of the local transfer current density (C/m^3)
R_s radius of positive electrode material (m)
S_e ratio of diffusion time versus discharge time
t time (s)
U open-circuit potential (V)
V cell potential (V)
V_c cutoff potential (V)
x distance from the separator/positive electrode boundary (m)

Greek letters

ϵ porosity of electrode
κ ionic conductivity of electrolyte (S/m)
σ electronic conductivity of solid matrix (S/m)
Φ electrical potential (V)

Subscripts

+ positive electrode
d discharge
r reaction zone
s separator or solid phase
T maximum concentration in intercalation material
1 solid matrix
2 solution phase

Superscripts

θ standard cell potential

Acknowledgements

This work was supported by the Assistant Secretary for Energy Efficiency and Renewable Energy, Office of Transportation Technologies, Electric and Hybrid Propulsion Division of the US Department of Energy under Contract No. DE-AC03-76SF00098.

Appendix

1. Parameters used in the model

We model a system with a lithium foil negative electrode, a solid polymer electrolyte separator, and a manganese dioxide composite positive electrode. The separator is an idealized polymer with a unity lithium-ion transference number, a conductivity of 4.0×10^{-5} S/cm, and a separator thickness of 10 μm.

In order to have a linear open-circuit potential variation with state-of-charge, we imagine cycling the manganese dioxide electrode over the limited range of $0.6\leqslant y\leqslant 0.8$ in $Li_yMn_2O_4$ (thus $k=0.03$). This leads to a capacity of $q=393.6$ C/cm^3; however, there is no way for the electrode to know that it is only to discharge in this range so we consider this to be a hypothetical situation. The initial open-circuit potential is 4.0 V, and the cutoff potential used is 2.0 V. The values of the electrode thickness ($L_+=40$ μm) and porosity ($\epsilon=0.14$) are obtained by maximizing the cell's specific energy for a three-hour discharge time.

References

[1] M. Doyle, T.F. Fuller and J. Newman, *J. Electrochem. Soc., 140* (1993) 1526.
[2] T.F. Fuller, M. Doyle and J. Newman, *J. Electrochem. Soc., 141* (1994) 1.
[3] T.F. Fuller, M. Doyle and J. Newman, *J. Electrochem. Soc., 141* (1994) 982.
[4] R. Selim and P. Bro, *J. Electrochem. Soc., 118* (1971) 829.
[5] G.W. Vinal, *Storage Batteries*, Wiley, New York, 4th edn., 1955.
[6] M.Z.A. Munshi and B.B. Owens, *Solid State Ionics, 38* (1990) 103.
[7] M. Doyle, T.F. Fuller and J. Newman, *Electrochim. Acta, 39* (1994) 2073.
[8] J. Newman and C.W. Tobias, *J. Electrochem. Soc., 109* (1962) 1183.
[9] W. Tiedemann and J. Newman, *J. Electrochem. Soc., 122* (1975) 1482.
[10] S. Atlung, B.Z.-Christiansen, K. West and T. Jacobsen, *J. Electrochem. Soc., 131* (1984) 1200.
[11] B.C. Knutz, K. West, B.Z.-Christiansen and S. Atlung, *J. Power Sources, 43/44* (1993) 733.
[12] J. Newman, *Electrochemical Systems*, Prentice-Hall, Englewood Cliffs, NJ, 1991.
[13] J. Newman, in R.E. White and J. Newman (eds.), *Proc. Douglas N. Bennion Memorial Symp.*, The Electrochemical Society Proceedings Series, Pennington, NJ, USA, 1994.